



저작자표시-비영리-변경금지 2.0 대한민국

이용자는 아래의 조건을 따르는 경우에 한하여 자유롭게

- 이 저작물을 복제, 배포, 전송, 전시, 공연 및 방송할 수 있습니다.

다음과 같은 조건을 따라야 합니다:



저작자표시. 귀하는 원저작자를 표시하여야 합니다.



비영리. 귀하는 이 저작물을 영리 목적으로 이용할 수 없습니다.



변경금지. 귀하는 이 저작물을 개작, 변형 또는 가공할 수 없습니다.

- 귀하는, 이 저작물의 재이용이나 배포의 경우, 이 저작물에 적용된 이용허락조건을 명확하게 나타내어야 합니다.
- 저작권자로부터 별도의 허가를 받으면 이러한 조건들은 적용되지 않습니다.

저작권법에 따른 이용자의 권리는 위의 내용에 의하여 영향을 받지 않습니다.

이것은 [이용허락규약\(Legal Code\)](#)을 이해하기 쉽게 요약한 것입니다.

[Disclaimer](#)

공학석사학위논문

**Effect of Organic Substrate Inflow
and Iron Oxides Transformation
on Arsenic Mobility in Soil
of Redox Transition Zone**

Redox Transition Zone 토양에서
유기물 유입과 철산화물의 성질 변화가
비소의 이동성에 주는 영향

2020년 2월

서울대학교 대학원

건설환경공학부

박수진

Abstract

Effect of Organic Substrate Inflow and Iron Oxides Transformation on Arsenic Mobility in Soil of Redox Transition Zone

Sujin Park

Civil and Environmental Engineering

The Graduate School

Seoul National University

Redox transition induced by change in hydrological regime has profound impact on biogeochemical reactions, which in turn altering As mobility. Changing As mobility in redox transition zone is a serious problem around the world, particularly in South Asia. However, few studies have demonstrated tendency of As mobility in repetitive redox conditions. By batch incubation test, this study extends the understanding of underlying biochemical reactions affecting As mobility in redox transition zone. Since As release is induced by microbial reductive dissolution of Fe and As, As speciation, crystallinity of Fe oxides, and soil bacterial communities were considered to be major factors affecting As mobility. Effect of organic

substrate (glucose) to As speciation was investigated. Results revealed that As released by biotic reductive dissolution in anoxic condition adsorbed to soil in the subsequent oxic condition, and the extent increased as the anoxic-oxic cycles repeated. The percentage of aqueous As in solution decreased from 25.2 to 11.9% at the end of 1st / 4th oxic cycle. However, As adsorption decreased again with $As(V)/As_{total}$ in solution when glucose was added. Since As(III) has lower affinity for minerals than As(V), this suggests that organic substrate can inhibit As adsorption by affecting its valence. Transformation of iron (hydr)oxides was corroborated by X-ray absorption near edge structure - linear combination fitting (XANES-LCF) and selective extraction of soil iron oxides. Ratio of ferrihydrite, which is representative short range ordered (SRO) Fe oxides, increased to 29.3% after three times of redox shifts. AAO extractable Fe (Ammonium oxalate extractable Fe: amorphous Fe) increased from 1.4 to 3.2 mg/g while DCB extractable Fe (Dithionite carbonate-bicarbonate extractable Fe: both amorphous and crystalline Fe) remained constant. This implies that Fe oxides transformed to amorphous form under repetitive redox changes. Since amorphous Fe oxides are much vulnerable to microbial reductive dissolution by their higher surface area and solubility, transformation of Fe oxides to amorphous form can lead to greater level of As release in anoxic condition. Bacterial communities were investigated with Illumina sequencing. Bacterial community changed actively to redox changes. Proportion of strict (an)aerobes gradually decreased, while microaerophilic

genus (*Azospirillum*) became the predominant genus making up 72.8% of total counts at the end of incubation. Some indigenous bacteria capable of Fe or As reduction (e.g. *Clostridium*, *Desulfitobacterium*) were dominant, which may facilitated As/Fe reduction. In conclusion, cumulative effects of redox shifts made As more mobile and toxic. Thus, long term monitoring is needed to manage As-contaminated redox transition zones.

Keywords: Redox transition zone, As release, Amorphous iron oxides, Fe reductive dissolution

Student Number: 2018-22553

Table of Contents

1. Introduction.....	1
1.1 Background.....	1
1.2 Research objectives	7
2. Materials and method	8
2.1 Materials	8
2.1.1. Soil characterization.....	8
2.1.2. Manufacture of artificially contaminated soil .	11
2.1.3. Preparation of artificial soil solution.....	11
2.2 Method.....	12
2.2.1. Soil incubation test.....	12
2.2.2. Aqueous chemistry analysis.....	13
2.2.2.1. Analysis of total As concentration.....	13
2.2.2.2. As speciation.....	14
2.2.2.3. Fe speciation.....	15
2.2.3. Investigation of Fe oxides transformation.....	16
2.2.3.1. AAO (Ammonium oxalate) extraction.....	16
2.2.3.2. DCB (Dithionite carbonate-bicarbonate)	
extraction	17

2.2.3.3. XANES-LCF analysis	17
2.2.4. Fractionation of As in soil	19
2.2.5. Bacterial community analysis	22
2.2.5.1. Illumina sequencing.....	22
2.2.5.2. Statistical analysis	23
3. Results and Discussion	25
3.1 Effect of organic substrate on As mobility	25
3.1.1. Arsenic Partitioning under Dynamic Redox Conditions.....	25
3.1.2. Effect of Organic Substrate on As Transformations	27
3.1.3. Decrease in binding strength of As by organic substrate	29
3.2 Transformation of Fe oxides to amorphous form...31	
3.2.1. XANES-LCF analysis	31
3.2.2. Selective extraction of soil iron oxides	33
3.3 Bacterial community analysis	39
3.3.1. Change in bacterial community	39
3.3.2. Decrease in microbial diversity	47

4. Conclusions	52
Reference	54
Abstract in Korean	66

Contents of Table

Table 2.1. Soil characterization	10
Table 2.2. Procedure for Wenzel 5-step sequential extraction	21
Table 3.1. Fe K-edge XANES linear combination fit results after different days of incubation.....	36
Table 3.2. The relative abundance of the dominant phylogenetic groups	44
Table 3.3. Summary of sequencing analysis of bacterial communities in the soil samples	50

Contents of Figures

Fig 1.1. Three possible mechanisms of arsenic mobilization in anoxic sub-surface aquifer materials as mediated by metal respiring bacteria	6
Fig 2.1. Schematic diagram for soil incubation.....	13
Fig 3.1. pH and Eh of soil solution under redox change.....	26
Fig 3.2. Aqueous As and percentage of As(V) in soil solution.....	26
Fig 3.3. Glucose in soil solution under repetitive redox change	29
Fig 3.4. Percentage of As fractions in incubated soil.....	31
Fig 3.5. Ammonium oxalate extractable and Dithionite carbonate-bicarbonate extractable Fe under redox change	32
Fig 3.6. Fe K-edge XANES spectra of the reference materials and soils	34
Fig 3.7. Fe K-edge XANES-LCF of the soil.....	35
Fig 3.8. Percentage of Fe oxides in soil under redox change.....	36
Fig 3.9. The changes in bacterial communities at the genus level.....	40
Fig 3.10. Heatmap analysis for bacterial communities at the genus level	40
Fig 3.11. Venn diagram showing overlap between species	47
Fig 3.12. Alpha-diversity indices of the samples.....	49
Fig 3.13. Principal component analysis of bacterial communities	51
Fig 3.14. Increased mobility of As under anoxic condition	53

1. Introduction

1.1 Background

Arsenic (As) is a carcinogen that causes severe health problem (Humans et al., 2004). Mine effluent, pesticide, and poultry waste are major sources for As-contaminated soil (Smedley and Kinniburgh, 2002, Winkel et al., 2008). In soil, most of As is adsorbed or co-precipitated to iron oxides, which has low mobility and toxicity (Mandal and Suzuki, 2002). There are various chemical form of As, but most of As exists in inorganic arsenite or arsenate in soil. It tends to be released and adsorbed depending on the redox status in soil. In reducing condition, Fe(III) is reduced to Fe(II) and solubilized from the surface of oxides (Harvey et al., 2002). Iron oxides-bound arsenic is then released together. This is termed reductive dissolution, which is the major source of groundwater contamination by As. When oxygen is reintroduced, Fe(II) rapidly precipitates on the surface of iron oxides as Fe(III) oxides and released As adsorb to them again. Amorphous iron oxides, whose representative mineral is ferrihydrite in soils and sediments, are easier to be reduced and exhibit higher adsorption capacity compared to crystalline iron oxides, such as hematite and goethite. This is

explained by their higher surface area and solubility (Schwertmann and Cornell, 2008). Therefore, properties of soil iron oxides play a key role on As partitioning.

Redox change also controls the speciation of As (i.e., As(V), As(III)), which in turn determines its toxicity and mobility (Benner, 2010). Since As(III) is uncharged at circumneutral pH, its binding affinity to Fe/Al oxides, calcium, and nonspecific sorption is lower than that of As(V). Therefore, it is known to be more mobile and toxic. In oxidizing condition, As(V) prevails while As(III) is dominant form in reducing condition thermodynamically. However, reaction rates of As(III) oxidation is extremely slow in natural environment and thus As typically coexists in HAsO_4^{2-} (As(V)), H_2AsO_3^- (As(V)), and H_3AsO_3^0 (As(III)) in general soil pH (Ferguson and Gavis, 1972). Reduction of iron and arsenic can occur thermodynamically when the Eh is below about 200 mV in the general soil pH range (5-8), but the reaction rate is very slow (Burnol et al., 2007). In the natural environment, microorganisms facilitate the transfer of electrons between the electron donor, the carbon source, and the electron acceptor, iron and arsenic (Newman and Banfield, 2002). Representative dissimilatory Fe / As reducing bacteria are *Shewanella*, *Geobacter*, and *Clostridium*, and many others (Dobbin et al., 1999, Lovley, 2006, Jiang et al., 2013). The

relative abundance and diversity of species that can use iron or arsenic as the electron acceptor in soil microbes has a significant impact on the behavior and bioavailability of the element (Lara et al., 2012). Soil microbial community is therefore a key determinant of arsenic mobility and toxicity.

When soil environmental condition changes, each microorganism succeeds or fails to adapt and the entire microbial community is constantly changing. Major environmental factors that may affect the microbial community include soil particle size, pH, Eh, and nutrients (Torsvik and Øvreås, 2002). Eh is one of the major environmental factors that greatly affect the microbial community. Changes in Eh affects the final electron acceptor available to microorganisms. Microbial community composition affects the circulation of major minerals such as carbon (C), sulfur (S), nitrogen (N), phosphorus (P), arsenic (As) and iron (Fe) in soils (Loreau, 2001, D'Hondt et al., 2004, Falkowski et al., 2008), studying of microbial community changes in the redox transition zone is useful for predicting and reducing hazards in arsenic-contaminated soils. To date, various studies have been carried out on the phenomenon of facilitated dissolution of arsenic by Fe/As reducing microorganisms (Islam et al., 2004, Wang et al., 2016, Wang et al., 2017, Yang et al., 2018). However, research on the trend of soil microbial community change at the interface of changing Eh is insufficient.

Some studies have analyzed microbial communities over time in soils with changing environmental conditions due to seasonal or tidal events (Boucher, et al., 2006, Waldrop and Firestone, 2006). However, the correlation between Eh and microbial community is not yet clear.

Soil redox condition changes when there is a change in hydrological regime (Clague et al., 2019). Submerged soil undergoes oxygen depletion, because water blocks the inflow of oxygen (Noël et al., 2019). Redox oscillating conditions are common in various near-surface environments, such as paddy soil, shallow aquifer with fluctuating water table, and site under hydrological management like managed aquifer recharge (Muntau et al., 2017, Lin et al., 2018, Clague et al., 2019). Redox transition zones are recently regarded as research area of high interest (Rodriguez-Mora et al., 2015, Bishop et al., 2019, Möller et al., 2019, Zhao et al., 2019), because geochemical reactions are facilitated by active microorganisms using various electron acceptors and donors (Lee et al., 2015). Recently, it has been reported that dissolved As concentration increases by seasonal variation in South Asia and United States (Jung et al., 2015, Meng et al., 2017, Xie et al., 2018, Duan et al., 2019). Arsenic release from soil to groundwater is a serious environmental problem and exposure to arsenic-contaminated groundwater can cause DNA damage and skin irritation on the receptors, as

well as cancers in the gastrointestinal tract, skin, bladder and liver (Calatayud et. al., 2014, Paul et al., 2015).

Whereas much studies have been conducted on As reductive dissolution, As mobility under dynamic redox conditions needs to be investigated more. Previous studies mostly focused on As release when oxygen is absent. Therefore, this study aims to assess the tendency of As mobility in redox oscillations. For this, we assumed that single redox cycle differs from multiple redox cycles and focused on the cumulative effect of them. To simulate conditions of redox transition zone and examine the cumulative effect, we conducted soil incubation test and four anoxic-oxic cycles were repeated. In dynamic redox conditions, both As release and adsorption were considered. Specifically, labile carbon source and transformation of Fe oxides in soil were considered to be main factors affecting biogeochemical reactions controlling As mobility. Also, this study aims to investigate the changes of bacterial community in soil environment where redox conditions continuously oscillate and to provide background data for predicting characteristics of arsenic leaching in the long term. Our approach will extend current understanding of the cumulative impacts of redox change on iron(III) (hydr)oxides transformation and As valence, resulting in increased risk of As in long-term.

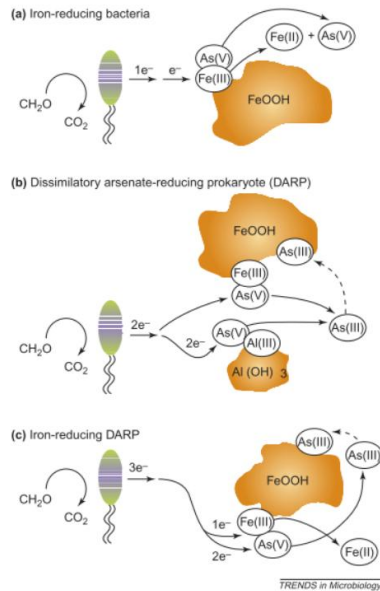


Fig 1.1. Three possible mechanisms of arsenic mobilization in anoxic subsurface aquifer materials as mediated by metal respiring bacteria. (a) Release of As(V) by iron-reducing bacteria. (b) Release of adsorbed arsenic from the surfaces of either Fe(III) or Al(OH)_3 minerals via reduction of As(V) to As(III) as mediated by DARPs. (c) Reductive release of As(III) and Fe(II) by iron-reducing DARPs. (Oremland and Stolz, 2005).

1.2 Research objectives

The objective of this research is to extend understanding of underlying biogeochemical reactions affecting As mobility in redox transition zones with fluctuating hydrological regime. Detailed objectives of the research are as follows:

- (1) To investigate potential effect of organic substrate, an electron donor for microbially mediated Fe/As reductive dissolution, to the valence and adsorption of As

- (2) To elucidate transformation of Fe oxides in soil under repetitive redox changes and its effect on As mobility

- (3) To investigate cumulative effect of redox transitions to the bacterial community structure in arsenic contaminated soil

2. Materials and method

2.1 Materials

2.1.1 Soil characterization

Natural soil was collected from the field site in Seoul, South Korea. It was collected at a depth of 0-30 cm and air-dried at the room temperature. Then the soil was passed through sieve to achieve particle size below 500 μm .

pH of soil was measured according to the Methods of Soil Analysis, Part 3-Chemical Methods (Sparks, Helmke, and Page, 1996). Soil slurry was manufactured at solid : liquid ratio of 1:5. Soil solution was separated using vacuum filter with 0.22 μm filter (Whatman, UK). Then pH of the soil solution was measured.

Elemental composition of the soil was determined by USEPA method 3052 (HNO_3 : HF : H_2O_2 : dH_2O , 9:3:1:1, v/v/v/v) (EPA, 1995). 1 g of soil was digested by microwave (MSP1000, CEM, USA) for 5.5 minutes to 180°C and maintained for 9.5 minutes. Supernatant was filtered using 0.45 μm filter. Metal concentration was measured by inductively coupled plasma optical emission spectrometer (ICP-OES, iCAP 7400 Series, Thermo Scientific, USA).

Ammonium oxalate (AAO) extractable Fe was determined by oxalate extraction method (Borggaard, 1979). The physicochemical properties of soil are shown in Table 2.1.

Bulk mineralogy of soil was analyzed by Powder XRD (D8 ADVANCE with DAVINCI, Bruker AXS, Germany). $\text{CuK}_{\alpha 1}$ radiation source was used. Intensities were recorded between a range of $3\text{-}70^\circ 2\theta$ with increments of $0.02^\circ 2\theta$. XRD results showed that the main crystalline phase of soil was quartz and albite. Iron oxides in soil were mainly composed of hematite and goethite. Bulk element composition was determined by X-ray fluorescence spectrometer (XRF; S4 PIONEER, Bruker AXS, Germany).

Table 2.1. Soil Characterization

pH	Texture	Fe (mg/g)	AAO extractable Fe (mg/g)	Ca (mg/g)	SiO₂ (%)	Al₂O₃ (%)	SO₃ (%)	Main crystalline phase
5.8	Sandy loam	14.09	1.44	2.17	57.95	29.98	0.14	Quartz, Albite

2.1.2 Manufacture of artificially contaminated soil

2 kg of air-dried soil was mixed with a solution of As(V) (sodium arsenate dibasic heptahydrate, $\text{HAsNa}_2\text{O}_4 \cdot 7\text{H}_2\text{O}$, Fluka, +98.0% purity) to achieve final concentration of 250 mg As(V)/kg soil. Contaminated soil was packed in plastic container and aged for 75 days without air contact at room temperature. This soil was referred to as 'original' soil.

2.1.3 Preparation of artificial soil solution

The properties of artificial soil solution medium followed that of Duan, which consists of pH 7.0, 10 mM PIPES, 2.7 mM KCl, 0.3 mM MgSO_4 , 7.9 mM NaCl, and 0.4 mM $\text{CaCl}_2 \cdot 2\text{H}_2\text{O}$ (Duan et al., 2019). 2 mM of glucose was amended at the beginning of 1st and 4th anoxic cycles. This is labile carbon source, which can act as an electron donor for microbial reductive dissolution.

2.2 Method

2.2.1 Soil incubation test

Soil incubation test was conducted to control soil redox condition over a 56 d duration (Couture et al., 2015). 10 g of dried soil was mixed with 200 mL of artificial soil solution medium in 250 mL serum vials. Incubations were conducted for 7 days in anoxic condition ensued by 7 days of oxic condition. Before the anoxic incubation, N₂ gas was purged for 15 minutes and sealed with Teflon-coated butyl rubber septa and aluminum crimp caps to prevent oxygen input. Sampling was carried out in anaerobic chamber. After 7 days, O₂ gas was purged at the bottom of the vial and kept for 7 days. Redox potential of the soil slurry kept higher than 300 mV during the oxic period. Samples were kept in the dark at 25°C. Anoxic-oxic cycles were repeated 4 times. Soil solution was sampled at 2, 4, 7 days of each cycle. Soil was sampled at the end of each incubation period by vacuum filtration. Sampled soil was kept at 4°C in the dark. Samples were termed as their last incubation periods. For example, soil sampled after 3rd oxic incubation was named “Oxic 3”. All experiments were performed in triplicate and samples were set separately for each cycle for soil sampling.

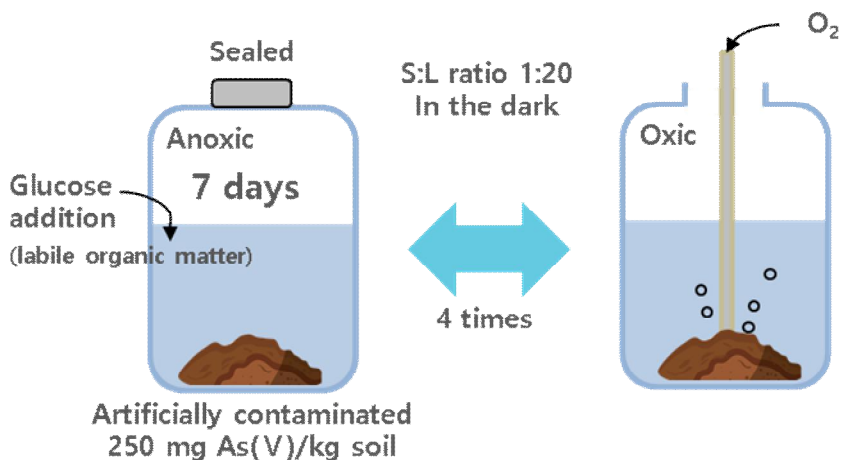


Fig 2.1. Schematic diagram for soil incubation

2.2.2 Aqueous chemistry analysis

2.2.2.1 Analysis of total As concentration

Sampling was conducted after 2, 4, 7 days of each incubation cycle. All the sampling was conducted in anaerobic chamber (VS-5600A, Vision Scientific, Korea) during the anoxic period. 5 mL of soil suspension was collected. Aliquots were filtered with 0.45- μm syringe filter, diluted, and acidified using 1% v/v nitric acid (HNO_3) for aqueous chemistry analysis. The concentration of arsenic was analyzed by ICP-OES or ICP-MS (G8421A, Agilent Technologies International, Japan). Detection limit of ICP-MS was 1 $\mu\text{g/L}$. Coefficient of determination of arsenic standards were

higher than 0.998.

Eh and pH were measured by combination meter (US/720A, Thermo Scientific, USA). Relative redox potential was measured by Ag-AgCl reference electrode. Glucose concentrations were measured enzymatically with the glucose (HK) reagent kit (Megazyme Co.) after the samples had been filtered.

2.2.2.2 As speciation

Colorimetric method was used for As(V) analysis (Hu, Lu et al. 2012). Molybdate blue reagent selectively forms complex with As(V), which as an α -Keggin structure. This anion is then reduced by ascorbic acid to form the blue colored β -Keggin ion.

3 mL of samples were acidified with 1% HCl. Acidified samples were mixed with 0.3 mL of deionized (DI) water. After 5 minutes, 0.3 mL of color reagent was added. 125 mL of 5 N sulphuric acid, 37.5 mL of ammonium molybdate solution, 75 mL of 0.1 M ascorbic acid solution, and 12.5 mL of potassium antimonyl tartrate solution were mixed thoroughly to make molybdate blue color reagent. The absorbance at 880 nm of mixed sample was measured after 5 minutes using spectrophotometer. Total As was

measured by ICP-OES or ICP-MS. The concentrations of arsenite and arsenate were calculated by following equation.

$$\text{As(III)} = \text{As}_{\text{total}} - \text{As(V)} \quad \text{Eq. 1}$$

2.2.2.3 Fe speciation

Measurement of ferrous iron was performed by ferrozine assay (Stookey, 1970). The chelator, 3-(2-pyridyl)-5,6-bis(4-pheylsulfonic acid)-1,2,4-triazine (Ferrozine), absorbs at 562 nm when bound to ferrous iron, allowing for quantification.

0.01 M of ferrozine was prepared in an 0.1 M ammonium-acetate ($\text{CH}_3\text{COONH}_4$) solution. 1.4 M of hydroxylamine hydrochloride ($\text{H}_2\text{NOH}\cdot\text{HCl}$) was prepared in hydrochloric acid solution of 2 M. Then buffer was produced by preparing 5 M ammonium acetate solution adjusted at pH 9.5 with a solution of ammonium hydroxide (28-30% NH_4OH). All samples were directly acidified with 0.5 M HCl to prevent reaction with oxygen. Deionized water, ferrozine solution, and buffer solution was mixed at ratio of 7.5:1:1.5 to make 'mix A' solution. Then, 100 μL of sample was amended in 4 mL of mix A solution. After 2-3 minutes, absorbance at 562

nm was recorded. Coefficient of determination of standard curve for ferrozine assay was higher than 0.99, and only the absorbance lower than 0.1 was recorded. If not, samples were diluted with 0.5 M HCl solution.

2.2.3 Investigation of Fe oxides transformation

2.2.3.1 Ammonium oxalate (AAO) extraction

Oxalate extraction was performed to estimate 'active' or 'non-crystalline' iron. 'Active' iron refers to iron that exists in non-crystalline forms and thus more reactive and amorphous minerals. These can be selectively extracted by ammonium oxalate solution in dark. Soil of < 0.063 mm was used for oxalate extraction. 100 mL of 0.2 M ammonium oxalate ($C_2H_8N_2O_4$) solution was mixed with 75 mL of 0.2 M oxalic acid ($C_2H_2O_4$) solution. pH was adjusted to 3 with the addition of ammonium oxalate.

Soil samples were collected at the end of aerobic incubation with vacuum filtration. All the released ferrous iron was immobilized again and thus total iron content remained constant. Soil was dried and 0.4 g was weighed. Weighed soil was mixed with 40 mL of oxalate reagent in 50 mL centrifuge tube. Tubes were covered in tin foil. Tubes were placed on horizontal shaker for 4 hours. After 4 hours, tubes were centrifuge on high

for 12 minutes. Supernatants were collected, filtered, and acidified until analysis.

2.2.3.2 Dithionite carbonate-bicarbonate (DCB) extraction

Dithionite citrate-bicarbonate (DCB) extraction dissolves both non-crystalline and crystalline iron oxides using dithionite, which is a powerful reductant. 0.4 g of dry soil was reacted with 0.4 g of dithionite in 40 mL of citrate-bicarbonate solution (Loeppart and Inskeep, 1996).

2.2.3.3 X-ray absorption near edge structure-linear combination fitting analysis (XANES-LCF)

X-ray absorption near edge structure – linear combination fitting was used to investigate the transformation of Fe oxides. Soil of < 0.063 mm was used for XANES analysis. The XANES spectra of the Fe K-edge were collected from the beamline 10C at the Pohang Accelerator Laboratory (PAL) in South Korea. Samples were analyzed in transmittance mode using Fe foil as a reference.

Model compounds were hematite (α -Fe₂O₃), goethite (α -FeOOH), and ferrihydrite [(Fe³⁺)₂O₃•0.5H₂O]. These were determined by XRD

analysis. Magnetite ($\alpha\text{-Fe}_3\text{O}_4$) was not detected in original soil by XRD. Ferrihydrite was selected as reference, because it is a representative of amorphous iron oxides in soil. Hematite (Red ferric oxide, Fe_2O_3 , Daejung, Chemical pure) and goethite (Ferric hydroxy oxide, approx. $\text{FeO}(\text{OH})$, Junsei, Chemical pure) were used as a reagent.

Ferrihydrite was synthesized by dissolving 40 g of $\text{Fe}(\text{NO}_3)_3 \cdot 9\text{H}_2\text{O}$ in 500 mL dH_2O , adding 330 mL of 1 M KOH, and adjusting pH to 7-8 (Schwertmann and Cornell, 2008). The mixture was stirred with magnetic bar at room temperature for 24 h. The precipitate was washed with distilled water and dried at room temperature. It was confirmed with XRD that precipitate was 2-line ferrihydrite, which shows two broad peak at $2\theta=34^\circ$ and 61° .

Goodness of fitting was evaluated using R-factor and reduced Chi-square (χ^2). R-factor is calculated as the sum of the squares of the difference between the fit and the data. Reduced Chi-square is defined as chi-squared per degree of freedom. Spectra of samples were quantified with that of reference using Athena software (Ravel and Newville, 2005).

2.2.4 Fractionation of As in soil

Wenzel five-step sequential extraction was conducted with soil after incubation to elucidate As distribution (Wenzel et al., 2001). This method helps to separate As fraction in soil by its binding strength. The higher the number of fractions, the stronger the As bond.

Five different extractants are used. Firstly, 0.05 M $(\text{NH}_4)_2\text{SO}_4$ is reacted with soil for 4 h. This step mainly extracts non-specifically bound As (Fraction 1). Then, 0.05 M $(\text{NH}_4)\text{H}_2\text{PO}_4$ was used to extract As, whose major chemical form is specifically bound As (Fraction 2). 0.2 M of NH_4 -oxalate buffer (pH 3.25) was added to the soils and reacted for 4 h in the dark on horizontal shaker. Amorphous Fe/Al oxides bound As is the major chemical form of released As in this step (Fraction 3). To extract As in fraction 4, whose major chemical form is crystalline Fe/Al oxides bound As, samples were treated with 0.2 M NH_4 -oxalate buffer and 0.1 M ascorbic acid (pH 3.25) for 30 min at 96°C in oil basin. Residual As (Fraction 5) was measured by total acidic dissolution suggested by USEPA 3052 method. Details of sequential extraction is shown in Table 2.2.

All sequential extraction was performed in triplicate. At the end of each step, samples were centrifuged at 1900 rpm for 15 minutes

(IECMULTI-RF, Thermo scientific, USA) and filtered through a 0.45 μm GHP-filter for analysis. As concentration of the sample was analyzed using an ICP-OES or ICP-MS. To present 100% stacked column graph, sum of absolute concentrations of each fraction except released amount was adjusted. Relative standard deviation(%RSD) was below 13%.

Table 2.2. Procedure for Wenzel 5-step sequential extraction (Wenzel et al. 2001)

Major chemical form	Extractant	Extraction conditions
Nonspecifically bound	0.05 M (NH ₄) ₂ SO ₄	4 h shaking at room temperature
Specifically bound	0.05 M (NH ₄) H ₂ PO ₄	16 h shaking at room temperature
Amorphous Fe oxides bound	0.2 M NH ₄ -oxalate buffer at pH 3.25	4 h shaking in the dark at room temperature
Crystalline Fe oxides bound	0.2 M NH ₄ -oxalate buffer + 0.1 M ascorbic acid at pH 3.25	30 min in oil basin at 96 °C
Residual	Mixture of 9 mL nitric acid, 3 mL hydrofluoric acid, 1 mL hydrogen peroxide, and 1 mL deionized water	0.5 g of soil Microwave aided digestion at 180 °C for 15 minutes

2.2.5 Bacterial community analysis

2.2.5.1 Illumina sequencing

Next generation sequencing was performed by Chunlab, Inc. (Seoul, Korea). DNA was extracted from 10 g of incubated soil using a FastDNA SPIN Kit for Soil (MP Biomedicals, USA). The extracted DNA was amplified using primers targeting the V3 to V5 region of 16S rRNA gene. The primer sequences were as follows: bacteria specific primers 341F (5'-TCGTCGGCAGCGTC-AGATGTGTATAAGAGACAG-CCTACGGGNGGCWGCAG - 3') and 805R (5'-GTCTCGTGGGCTCGG-AGATGTGTATAGAGACAG-GACTACHVGGGTATCTAATCC - 3'); archaea specific primers A519F-Mi (5'-TCGTCGGCAGCGTC-AGATGTGTATAAGAGACAG-CAGCCGCCGCGGTAA) and A958R-Mi (5'-GTCTCGTGGGCTCGG-AGATGTGTATAAGAGACAG-YCCGGCGTTGAMTCCAATT - 3'); Amplifications were carried with initial denaturation at 95°C for 3 min, followed by 25 cycles for 30 s. 25 cycles of annealing at 55°C and extension at 72°C for 30 s were followed. Final extension was carried out for 5 min at 72°C. PCR reactions contained 2.5 mM dNTPs (2.5 µL), 10X buffer (2.5 µL), 1 uL of each primer, DNA (2 uL), and TaKaRa Ex Taq DNA polymerase (0.25 µL) in 25 µL mixtures. Condition of DNA was confirmed

by using 1% agarose gel electrophoresis and visualized by spectrometer. Illumina sequencing (Miseq) and Agilent 2100 Bioanalyzer System was used. Operational taxonomic units (OTUs) and rarefaction curves were generated with an identity cut off of 97%. For genus level, relative abundance was calculated as the number of counts divided by total counts per samples (%).

2.2.5.2 Statistical analysis

To compare the differences of bacterial communities between soils, statistical analysis was used. To determine core bacterial OTUs, Venn diagram was calculated using *Venn diagram package* of R program. Four kinds of alpha-diversity indices were calculated: Abundance-based coverage estimators (ACE), Jackknife, Chao 1, and phylogenetic diversity. ACE, Jackknife, and Chao 1 are related to the species 'richness' of the samples. These are diversity indices estimated from the ratio of rare OTUs (singleton and doubleton). The higher this proportion is, the greater the estimate of the diversity index is, as there are many undetected species. Phylogenetic diversity implies the species 'diversity' of them. This is calculated by summing the shortest distance between the nodes in phylogenetic tree. Principal component analysis (PCA) with STATA program was conducted to

monitor the similarities between different soils.

3. Results and discussion

3.1 Effect of organic substrate on As mobility

3.1.1 Arsenic partitioning under dynamic redox conditions

Over the four cycles, reducing conditions were confirmed by decline in Eh and pH, and increase in Fe(II) in solution, while inverse trends were observed in oxidizing conditions (Figure 3.1). Decrease in pH is may be due to the organic acid production by fermentative Fe/As reducing microorganisms such as *Clostridium* (Li et al., 2017). *Clostridium* was the predominant bacterial genus under anoxic status indeed (4.6-34.1% of relative abundance). Figure 3.2A shows aqueous As concentration in the control (circle) and glucose-spiked sample (square). Arsenic concentration was expressed in percentage, and 100% is arsenic mass of initially contaminated soil (250.1 mg/kg). In general, As concentrations were higher in anoxic condition and got lower in the following oxic condition. Under anoxic condition, ferrous iron was measured in the soil solution (1.0-5.9% of total iron), which implicates that reductive dissolution of iron (hydr)oxides affected As mobility.

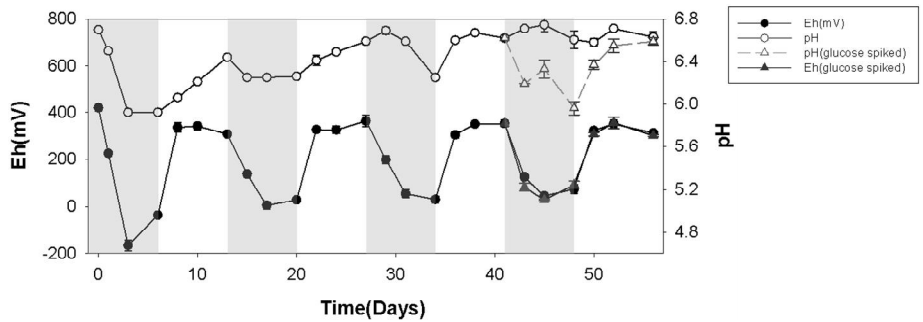


Fig 3.1. pH and Eh of soil solution under redox change

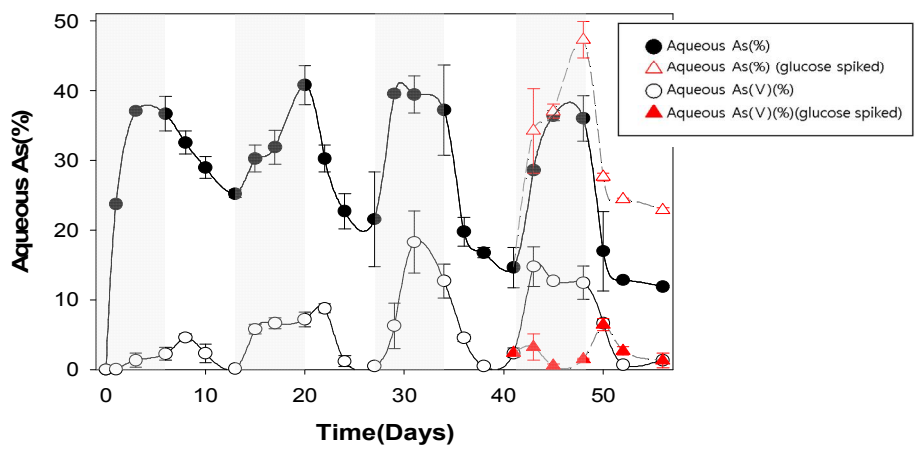


Fig 3.2. Aqueous As and percentage of As(V) in soil solution

After four repetitions of anoxic-oxic cycles, aqueous As in oxic cycle decreased from 25.2 (1st oxic), 21.6 (2nd oxic), 14.6 (3rd oxic) to 11.9% (4th oxic cycle). There was no considerable difference in aqueous As in anoxic condition. However, when glucose was spiked, decrease in As adsorption was evident and 22.9% of As was found to be in soil solution (4th oxic cycle). Additionally, As release during anoxic period significantly increased, resulting in 47.3% of aqueous As in 4th anoxic condition. Therefore, As adsorption increased as the redox cycle repeated, but input of exogenous carbon source increased As mobility again. Valence of arsenic was measured in order to delineate the impact of organic substrate on As partitioning.

3.1.2 Effect of Organic Substrate on As Transformations

Given that aqueous As in oxic condition increased as the glucose added, the oxidation state of As was identified to interpret this trend. As(III) was dominant form in overall incubation (Figure 3.2B), which confirmed the results reported in the literature, that As had a very low rate of oxidization in natural environment even though oxygen was purged (Ferguson and Gavis, 1972). This means that As in redox transition zones would exist in As(III) and would be highly mobile than expected. Unlike As(III), As(V) was almost

removed after 7 days of oxic incubation, which reflects higher sorption capacity of As(V) compared to As(III). PZC (Point of Zero Charge) values of iron oxides are above 7. Since pH in this experiment (pH 6-7) is lower than PZC value of iron oxides, surface of iron oxides is positively charged and preferentially attracts anions. Thus, affinity to iron oxides of As(V) (H_2AsO_4^- , HAsO_4^{2-}) (anionic) would be higher than that of As(III) (H_3AsO_3) (uncharged).

As glucose concentration in soil solution decreased (Figure 3.3), As(V)/As(total) in anoxic solution increased from 6.1 to 34.6% at the end of 1st / 4th anoxic cycle (Figure 3.2B). Ratio for As adsorption in each cycle (amount of adsorbed As under oxidizing conditions to aqueous As under reducing conditions) increased from 31.2 to 67.0%. On the other hand, the addition of glucose significantly decreased the concentration of As(V) in the aqueous solution again. This indicates that increase of As(V) under anoxic status must be due to the depletion of glucose, an electron donor for biotic As reduction. Since As(III) has lower affinity for Fe minerals than As(V), it is likely that increased proportion of As(III) in soil solution led to lower extent of As adsorption in oxic period when glucose was spiked. Therefore, change in As adsorption can be partly explained by valence of As. This suggests that labile soil organic matter not only promotes As reductive dissolution as reported in several studies (Parsons et al., 2013, Duan et al., 2019,

Bhattacharyya et al., 2018), but also inhibits readsorption of As by facilitating its reduction to As(III), which in turn increases As mobility.

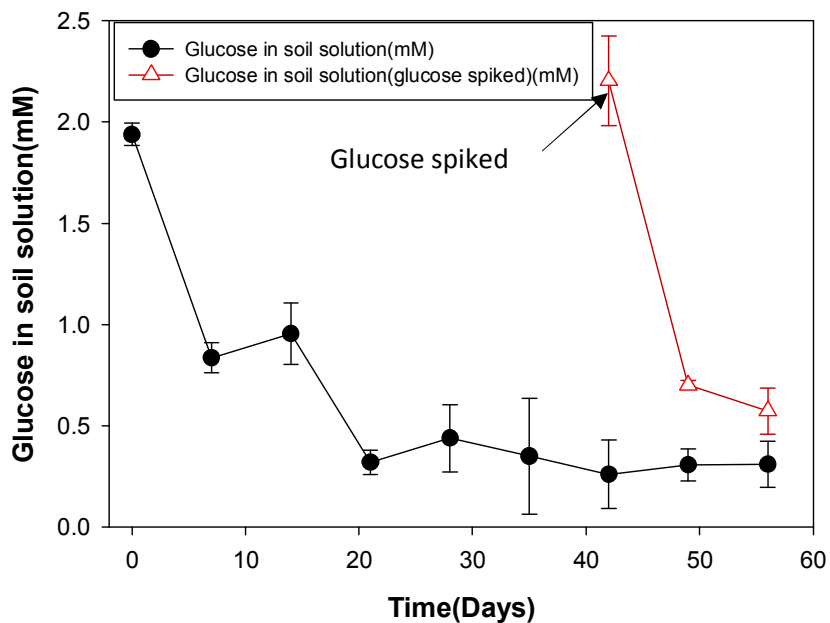


Fig 3.3. Glucose in soil solution under repetitive redox change

3.1.3 Decrease in binding strength of As by organic substrate

Wenzel 5-step sequential extraction was performed with soil after 1st, 4th, and glucose spiked 4th oxic incubation to compare binding strength of As. Generally, As of fraction 1 (F1) and 2 (F2) are considered labile and bioavailable (Kim et al., 2014). On the other hand, fraction 3 (F3), 4 (F4),

and 5 (F5) represents strongly bound As. As shown in the Figure 3.4, sum of F3, F4 and F5 increased from 53.6 to 65.2% as the cycle repeated. It decreased to 52.5% when glucose was spiked, which means presence of glucose weakened the binding strength of As to soil. Specifically, As of F3, whose major chemical form is amorphous Fe or Al oxides bound, showed the largest difference. As of F3 was 32.2 and 39.9% respectively in oxic 1 and oxic 4 soil (Figure 3.4). Slight increase might be due to the Fe oxides transformation to amorphous form which was proved above. When glucose was spiked, As of F3 decreased significantly to 22.4%. As of F4, whose major chemical form is crystalline Fe or Al oxides bound As, showed small increase. This is acceptable, because part of Fe oxides would become crystalline over time by Ostwald ripening. Residual fraction of As remained constant.

Decrease in binding strength of As by organic substrate might be resulted from decrease in As(V) in solution. As(V) forms inner-sphere bidentate binuclear-bridging complex with iron oxides, while As(III) forms inner-sphere monodentate complex or outer-sphere complex (Yoon, Park et al. 2016). In conclusion, not only sorption affinity to Fe oxides, but binding strength of As(III) is weaker than that of As(V). Although glucose-spiked 4th oxic soil contained considerable amount of HFO, As of F3 was the

lowest among the three samples. This implicates that valence of As in solution plays more significant role in As binding strength rather than crystallinity of soil Fe oxides.

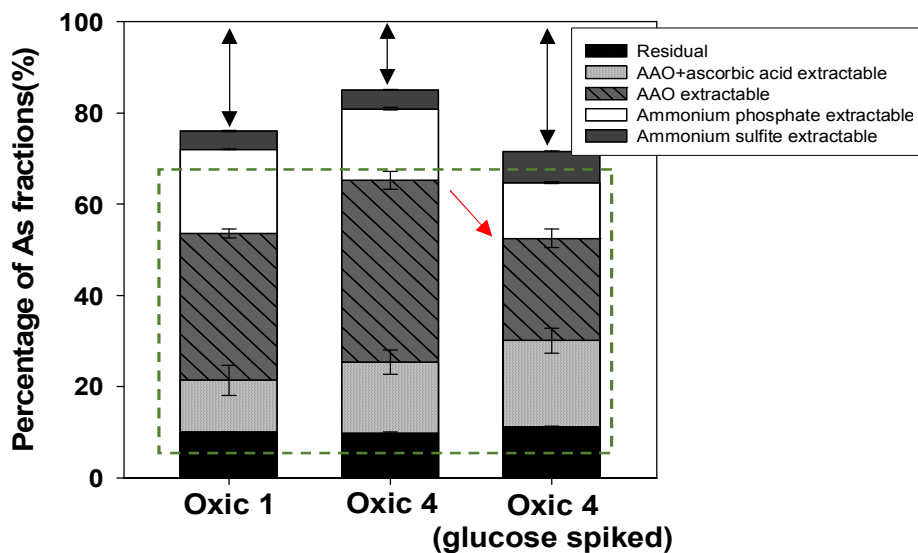


Fig 3.4. Percentage of As fractions in incubated soil

3.2 Transformation of Fe oxides to amorphous form

3.2.1 Selective extraction of soil iron oxides

AAO extractions were designed to selectively dissolve labile Fe oxides. AAO extractable Fe also increased from 1.4 to 3.2 mg/g under a series of redox cycles. DCB extractable Fe showed insignificant change, which

means that amount of total Fe oxides has not changed. Measured values describe that Fe redox changes promote the transformation of Fe oxides to amorphous varieties. This is consistent with the recent research which found that frequent shifts in redox conditions increased Fe(III) reactivity (Ginn et al., 2017). They observed that Fe(II) production increased under repetitive redox changes. This study additionally confirmed increase in Fe oxides reactivity with selective extraction.

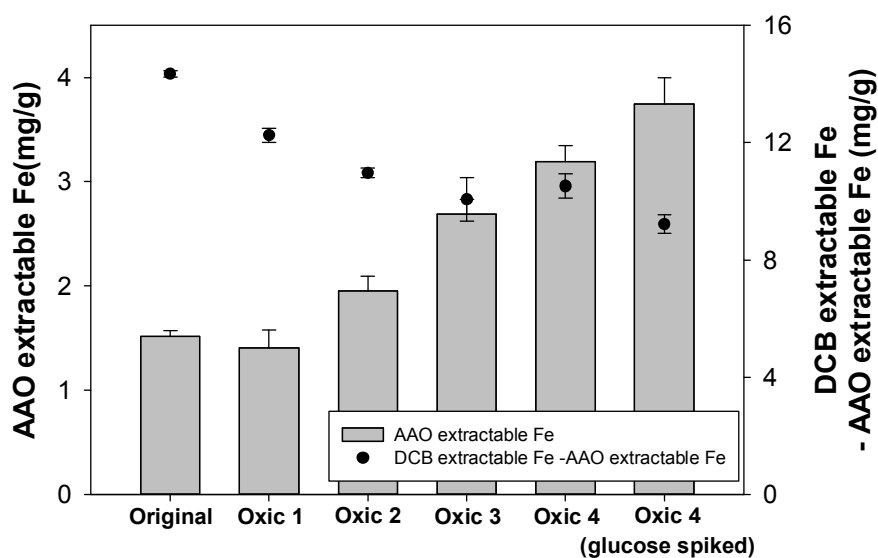


Fig 3.5. Ammonium oxalate extractable and dithionite carbonate-bicarbonate extractable Fe under redox change

3.2.2 XANES-LCF analysis

X-ray absorption near edge structure – linear combination fitting (XANES-LCF) was carried out to investigate compositional change in soil Fe oxides. LCF results show discernible change in the relative abundance of Fe oxides. LCF-weighted components are plotted in Figure 3.7 and fitting parameters are given in Table 3.1. As shown in Figure 3.8, original soil was composed of hematite (54%) and goethite (46%). However, after being exposed to consecutive redox changes, the fraction of ferrihydrite increased to 29.3% (Figure 3.8), while that of hematite decreased to 26.7%. According to X-ray photoelectron spectroscopy (XPS) and XANES-LCF, FeO, FeS, and Fe₃O₄ (magnetite) were not detected. Note that order of crystallinity is as follows: hematite, goethite, ferrihydrite (Schwertmann and Cornell 2008). Therefore, crystallinity of soil Fe oxides decreased when soil was subjected to repetitive redox changes. Hydrated Fe oxides (HFO) form weaker surface complexes with As (Dzombak and Morel, 1990), thus are more vulnerable to microbially catalyzed reductive dissolution during the anoxic period, thereby resulting in higher amount of As release (Mejia et al., 2016).

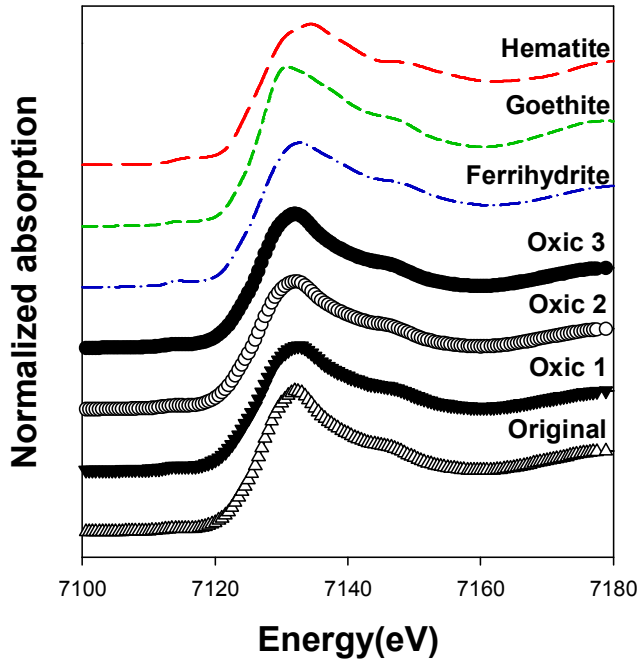


Fig 3.6. Fe K-edge XANES spectra of the reference materials (hematite, goethite, ferrihydrite) and soils (Original, Oxic 1, Oxic 2, Oxic 3)

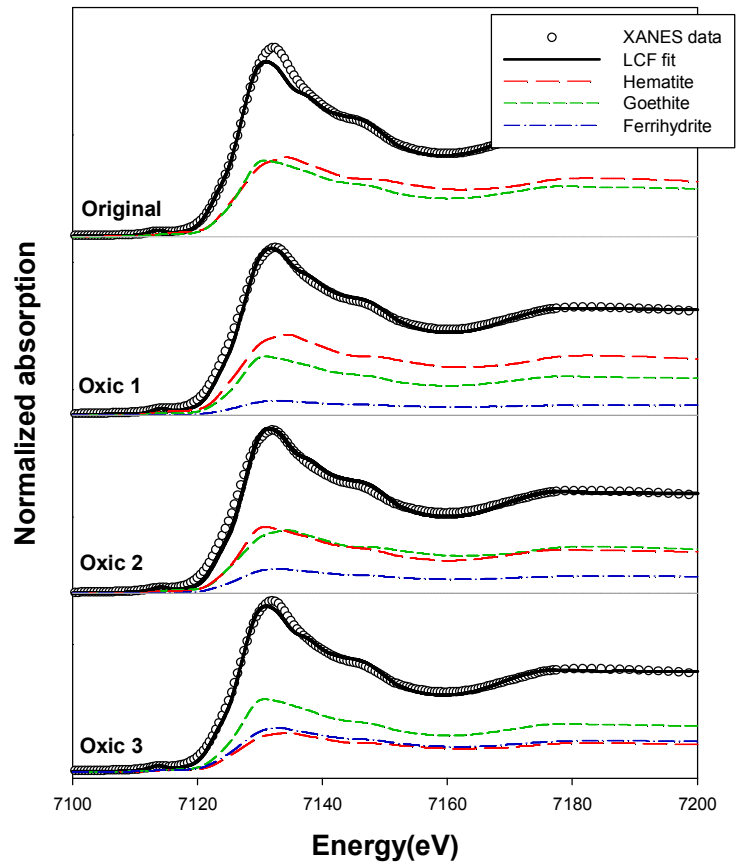


Fig 3.7. Fe K-edge XANES-LCF of the soil

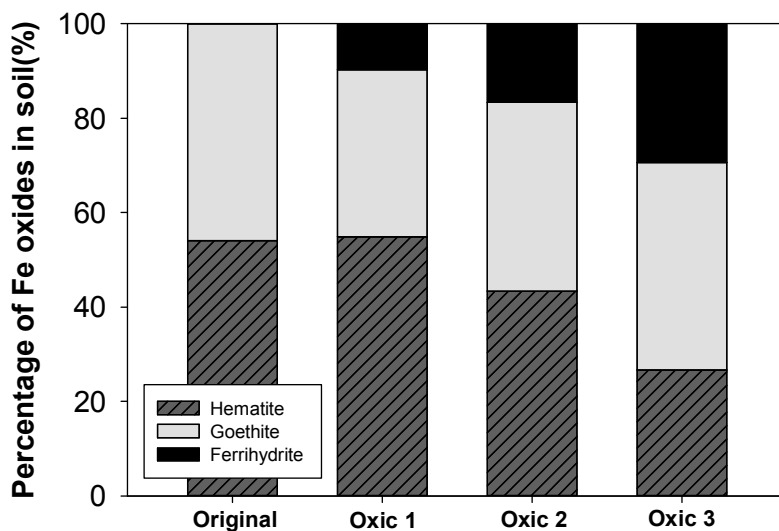


Fig 3.8. Percentage of Fe oxides in soil under redox change

Table 3.1. Fe K-edge XANES linear combination fit results after different days of incubation

Samples	Days (after)	Hematite Goethite Ferrihydrite			R-factor	Reduced chi- square
		-----(%)-----				
Original	0	54	46	0	0.008989	0.003418
Oxic 1	14	54.9	35.4	9.6	0.004595	0.001463
Oxic 2	28	43.3	40.1	16.6	0.009778	0.003234
Oxic 3	42	26.7	43.9	29.3	0.004282	0.001505

Ferric iron precipitates in hydrated form in natural environment, because hydrated solids have low interfacial nucleation energy (Stumm and Morgan, 1996). However, increase in amorphous Fe oxides accompanied with decrease in crystalline Fe oxides cannot be simply attributed to accumulation of hydrous Fe oxides followed by Fe reductive dissolution. Since crystalline Fe oxides such as hematite are greatly difficult to be reduced, there might be other reason with respect to the decrease of them. Transformation of Fe oxides is may be because of the (1) neof ormation of short-range-ordered (SRO) Fe-oxides on the surface of crystalline minerals. Ferric iron would be accumulated on the surface of the crystalline iron oxides in hydrous form, altering its surface to heterogeneous form. This may have been recognized as SRO Fe-oxides in XANES analysis. Other possible mechanism is (2) organic acid chelating Fe oxides. Fermentative iron reducing organisms produce organic acid such as acetate and lactate, using Fe(III) oxides as an electron sink for fermentation (Dong et al., 2016). *Clostridium*, which was predominant genus in this experiment, is a representative of fermentative Fe/As reducing bacteria (List et al., 2019). Produced organic acids act as chelating agents for both amorphous/crystalline iron oxides, increasing their extractability and surface heterogeneity (Lindsay, 1991). This can lead to the transformation of long-range ordered oxides (LRO) to SRO. HFO are highly

reactive and vulnerable to the reductive dissolution under anaerobic conditions. In conclusion, redox oscillations would increase As mobility in anaerobic conditions by decreasing crystallinity of Fe oxides. Without redox change, crystallinity of soil iron oxides increases by Ostwald ripening, which leads to lower degree of Fe and As release in reducing condition (Lee et al. 2019).

Whether frequent redox shifts transform Fe oxides to amorphous form is controversial yet. There are several studies showing that soil redox oscillations enhance crystallinity of iron oxides (Thompson et al., 2006, Parsons et al., 2013, Burnol et al., 2007, Kocar et al., 2006). They mention that crystallinity increases because Fe-O or Fe-S production under anoxic status followed by oxidation to well crystallized minerals (e.g., goethite, magnetite) accelerates Ostwald ripening. Soil used in this study had very low level of sulfur and moderate level of organic content (2.6%), so geochemical properties of soil might have influenced the transformation of Fe oxides. Therefore, change in the properties of Fe oxides seems to be related to the geochemical properties of the soil. Additional research on relationship of soil characteristics and Fe oxides transformation are needed.

3.3 Bacterial community analysis

3.3.1 Change in bacterial community

Original, Oxidic 1, Anoxic 2, Anoxic 3 and Anoxic 4 soils were sampled and analyzed with Illumina sequencing to monitor the response of the bacterial communities under repeated redox conditions. The relative abundance of the bacterial community at the genus level, heatmap analysis results, and the role of the bacterial genus reported in previous studies are shown in Figure 3.7. and Figure 3.8, respectively. In Figure 3.7, the group that accounts for less than 2% of the total counts was classified as 'Others'. Figure 3.8 shows the role and abundance of the 15 most abundant genera in all soil samples. The total number of reads for each sample identified at the species level based on 97% similarity was 58,813, 61,582, 50,160, 72,741, and 63,540, respectively. In each sample, the rarefaction curves showed similar trends, which approach to the saturation phase. Goods's coverage of library was 99.7% in all samples, indicating that almost all species were identified.

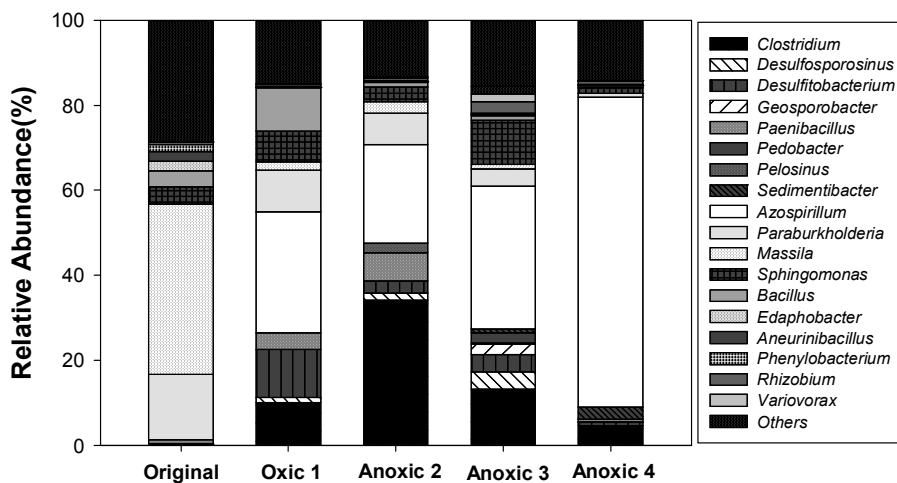


Fig 3.9. The changes in bacterial communities at the genus level

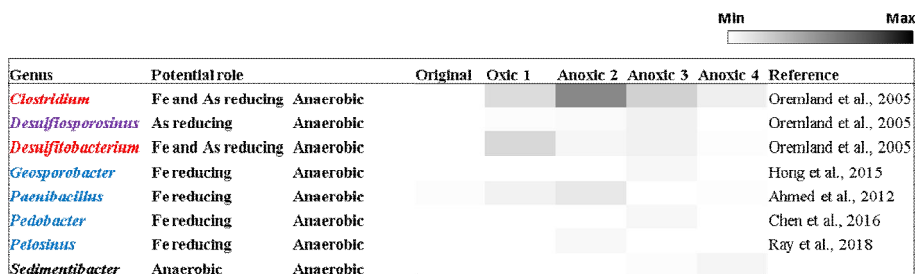


Fig 3.10. Heatmap analysis for bacterial communities at the genus level

The relative abundance of the bacterial community in each sample is summarized in Table 3.2. The major phylum of all soil samples was *Proteobacteria* (44.2-78.6%) and *Firmicutes* (11.4-53.0%). At the class level, *Betaproteobacteria* (1.3-58.6%) decreased significantly over time, whereas

Alphaproteobacteria (17.3-77.2%) increased gradually. Other classes included *Bacili* (1.3-14.7%) and *Clostridia* (1.2-30.0%). At the Order level, *Burkholderiales* (1.3-58.9%), *Bacilales* (1.3-14.7%), *Rhizobiales* (1.8-6.3%), *Rhodospirillales* (2.7-73.3%), *Clostridiales* (1.2-40.3%), and *Sphingomonadales* (1.5-11.0%) were dominant. At the family level, various microorganisms existed. *Oxalobacteraceae* (0.2-41.7%) including *Massila* (40.1%), an aerobic genus, was the most abundant in original soil, and *Rhodospirillaceae* (1.1-73.1%) was the most abundant in incubated soils. At the genus level, it was confirmed that the bacterial community in the soil changed in accordance with the redox change. Among the major genus, *Bacillus*, *Paenibacillus*, *Rhizobium*, *Rhodococcus*, and *Sphingomonas* are known to be resistant to trivalent or pentavalent arsenic (Jackson, Dugas et al., 2005, Bachate, Cavalca et al., 2009, Oliveira, Pampulha et al., 2009).

In incubated soils, various microorganisms known to be capable of Fe/As reduction, such as *Clostridium*, *Desulfosporosinus*, *Geosporobacter*, *Desulfitobacterium*, *Paenibacillus*, *Pedobacter*, *Pelosinus*, were found, and *Clostridium* (4.6-34.1%) was the most abundant genus among them (Ahmed, Cao et al., 2012, Hong, Kim et al., 2015, Ray, Connon et al., 2018). *Clostridium* is a microorganism that produces organic acid by fermentation and can reduce ferric iron. They are usually found in redox transition zones

(Wang, Yang et al., 2009, Mejia, Roden et al., 2016). Both amorphous and crystalline iron oxides can be used as electron acceptors, but rather, they promote iron reduction by flowing electrons through humic acids (Benz, Schink et al., 1998). Under four reduction conditions, the pH of the soil solution decreased to 5.9-6.3, and it is likely due to the production of organic acid by fermentative Fe/As-reducing microorganisms such as *Clostridium*. Except for *Rhodococcus*, which is known to oxidize trivalent arsenic, it is not known whether the top 15 genus microorganisms can oxidize divalent iron and trivalent arsenic. However, *Burkholderia* genus, similar to *Paraburkholderia*, has been reported to be capable of arsenic oxidation in previous studies (Sultana, Vogler et al., 2012).

Azospirillum is a nitrogen fixing microaerophilic microorganism that can be active under both reducing and oxidizing conditions (de Zamaroczy, Delorme et al., 1989). It was the most abundant genus in Oxidic 1 (28.5%), Anoxic 3 (33.6%), and Anoxic 4 (72.8%) soil, and its relative abundance gradually increased as the cycle was repeated. Absolute (an)aerobic microorganisms, on the other hand, gradually decreased as the redox change was repeated. This is because microorganisms which can only survive under certain redox conditions (i.e., *Massilia*, *Clostridium*), lose their activity because the redox environment is constantly changing.

Comparing the oxidized soil (Oxic 1) and reducing soil (Anoxic 2), it was confirmed that the Fe/As reducing microorganisms increased when the reducing conditions were formed as in the previous study (Parsons, Couture et al., 2013). Clostridium was only 10.1% in oxic 1 soil but increased by 34.1% in anoxic 2 soil. Fe/As reducing microorganisms, such as *Paenibacillus*, *Desulfosporosinus*, and *Pelosinus*, also increased in the reducing conditions. The increase of iron reducing microorganisms under reducing conditions is thought to promote the release of iron. Divalent iron was not detected in the soil solution under oxidizing conditions, but 1.0-3.3% of the total iron was released into the solution under reducing conditions. Strict (an)aerobic microorganisms have been found in all soils. This is because even strict (an)aerobic microorganisms require temporary reducing/oxidizing conditions for constant metabolism in natural environments (Teh, Silver et al., 2005). Moreover, it takes microorganisms considerable time to adapt to the Eh changes (DeAngelis, Silver et al., 2010).

Table 3.2. The relative abundance of the dominant phylogenetic groups

Sequences	Relative abundance (%)				
	Original	Oxic 1	Anoxic 2	Anoxic 3	Anoxic 4
(a) Phylum					
<i>Proteobacteria</i>	77.2	54.9	44.2	60.4	78.6
<i>Firmicutes</i>	11.4	41.0	53.0	33.0	19.2
Others	11.4	4.1	2.8	6.6	2.2
(b) Class					
<i>Betaproteobacteria</i>	58.6	14.2	13.0	7.8	1.3
<i>Alphaproteobacteria</i>	17.3	40.0	30.5	52.4	77.2
<i>Bacili</i>	9.8	14.7	8.2	1.9	1.3
<i>Clostridia</i>	1.2	24.0	40.3	30.0	14.6
Others	13.1	7.1	8.0	7.9	5.6
(c) Order					
<i>Burkholderiales</i>	58.9	14.2	13.0	7.7	1.3
<i>Bacillales</i>	9.8	14.7	8.1	1.9	1.3
<i>Rhizobiales</i>	6.0	2.6	2.5	6.3	1.8
<i>Rhodospirillales</i>	2.7	29.3	23.7	34.1	73.3
<i>Clostridiales</i>	1.2	24.0	40.3	30.0	14.6
<i>Sphingomonadales</i>	4.1	7.3	3.4	11.0	1.5
Others	17.3	7.9	9.0	9.0	6.2
(d) Family					
<i>Oxalobacteraceae</i>	41.7	3.9	4.9	1.4	0.2
<i>Burkholderiaceae</i>	16.2	9.9	7.6	4.1	0.9
<i>Rhodospirillaceae</i>	1.1	29.0	23.5	34.0	73.1
<i>Desulfitobacterium_f</i>	0.1	12.5	4.5	4.8	1.9
<i>Bacillaceae</i>	3.7	10.2	1.2	1.0	0.4

<i>Clostridiaceae</i>	0.3	10.1	34.1	15.5	6.9
<i>Sphingomonadaceae</i>	4.1	7.3	3.4	11.0	1.5
<i>Paenibacillaceae</i>	3.6	4.3	6.8	0.6	0.7
Others	29.2	12.8	14.0	27.6	14.4
(e) Genus					
<i>Massilia</i>	40.1	1.9	2.8	1.2	0.1
<i>Paraburkholderia</i>	15.3	9.8	7.4	4.0	0.9
<i>Azospirillum</i>	0.0	28.5	23.1	33.6	72.8
<i>Desulfotobacterium</i>	0.0	11.4	2.8	0.7	0.8
<i>Bacillus</i>	3.7	10.2	1.2	1.0	0.6
<i>Clostridium</i>	0.3	10.1	34.1	13.2	4.6
<i>Sphingomonas</i>	4.1	7.3	3.4	10.4	1.3
<i>Paenibacillus</i>	1.0	3.9	6.7	0.3	0.6
<i>Desulfosporosinus</i>	0.0	1.1	1.7	4.1	1.1
<i>Geosporobacter</i>	0.0	0.0	0.0	2.5	0.1
Others	35.5	15.8	16.8	29	17.1
(f) Species					
<i>Massilia arvi</i> group	28.5	0.1	0.1	0.2	0.0
<i>Massilia aerilata</i> group	8.6	0.3	0.0	0.8	0.0
<i>Paraburkholderia caledonica</i> group	8.1	0.0	0.1	0.8	0.2
<i>Paraburkholderia dipogonis</i> group	0.0	8.3	3.6	0.0	0.0
<i>Azospirillum oryzae</i> group	0.0	28.5	23.0	33.5	72.7
<i>Sphingomonas pruni</i> group	0.0	7.1	3.4	10.1	1.2
<i>Sphingomonas lutea</i> group	3.6	0.0	0.0	0.2	0.0
<i>Clostridium magnum</i>	0.0	2.9	22.7	0.0	0.0
<i>Clostridium beijerinckii</i>	0.0	2.8	2.4	10.1	3.4

<i>group</i>					
<i>Geosporobacter</i> <i>subterraneus group</i>	0.0	0.0	0.0	2.5	0.1
<i>Desulfitobacterium</i> <i>dichloroeliminans</i>	0.0	11.1	2.7	0.0	0.1
<i>Paenibacillus borealis group</i>	0.0	2.2	3.9	0.0	0.0
Others	51.2	36.7	38.1	41.8	22.3

3.3.2 Decrease in microbial diversity

As a result of Venn diagram analysis (Figure 3.9), 186 OTUs were common to all samples, and among them, the bacterial community of 0.5% or more abundance in incubated soil was determined as the core bacterial community (Shade and Handelsman 2012). The *Azospirillum oryzae* group and the *Clostridium beijerinckii* group capable of reducing Fe and As were core bacterial community (Dobbin et al. 1999).

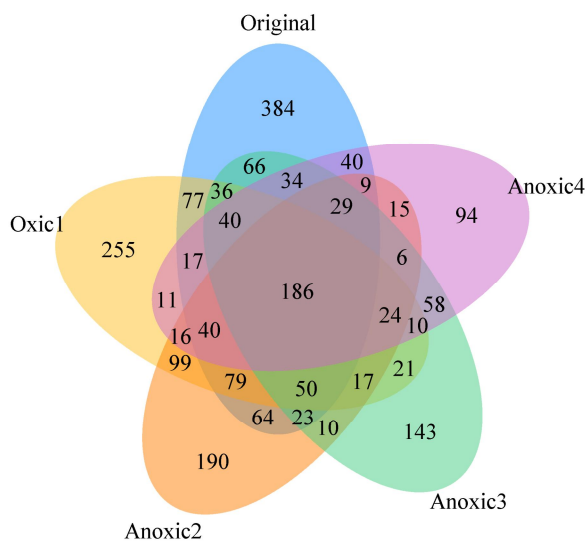


Fig 3.11. Venn diagram showing overlap between species

To analyze the effect of redox changes on the diversity of soil bacterial communities, the alpha-diversity indices in each soil were

compared. Based on 97% similarity, OTU tends to gradually decrease from 1,834 (Original), 1,088 (Oxic 2), 962 (Anoxic 2), and 1,024 (Anoxic 3) to 772 (Anoxic 4) in four redox cycles. Diversity indices such as ACE, Chao 1, and Jackknife are shown in Table 3.3. The values of ACE, Chao 1, and Jackknife have positive correlations with richness of species. Phylogenetic diversity is an index that quantifies the systematic differences between species by summing the shortest distances between nodes in the phylogenetic tree. All diversity indices declined significantly with repeated redox changes, highest in original soils and lowest in Anoxic 4 soils (Figure 3.10). Jackknife declined sharply from 2018 to 950, Chao 1 from 1,868 to 848, and phylogenetic diversity from 1,926 to 1,121. This means that when Eh changes repeatedly, strict (an)aerobes lose their activity, and the diversity of soil bacterial communities can be reduced. As a result of Venn diagram analysis, the number of species detected in only one sample decreased from Original (384), Oxic 1 (255), Anoxic 2 (190), and Anoxic 3 (143) to Anoxic 4 (94) with species diversity over time.

De Angelis et al. (2010) showed that diversity of microbial communities is higher under Eh changes rather than constant Eh with soil incubation test. This study extended it by showing that bacterial diversity decreased when redox change repeated. The high diversity of microbial

communities means that microorganisms with diverse functions are active and can utilize soil elements efficiently (Loreau, 2001). Thus, the reduction of microbial diversity due to repeated redox changes may inhibit the effective circulation of various inorganic substances in the soil (Torsvik and Øvreås, 2002).

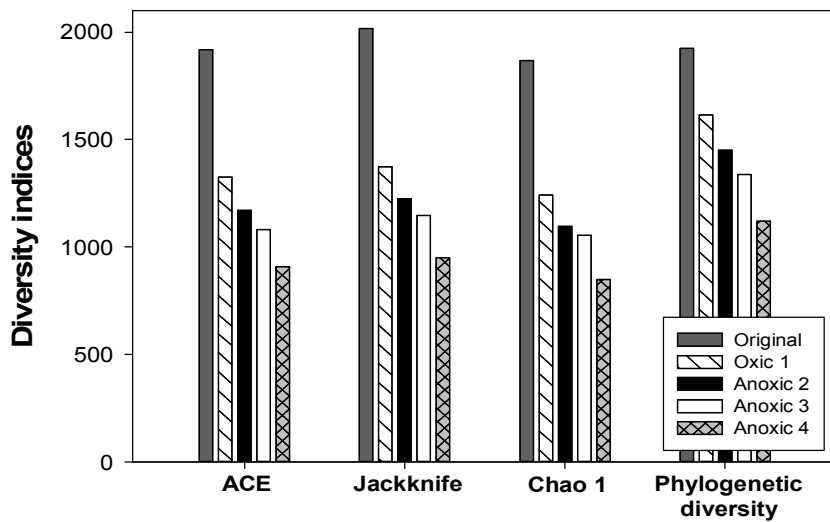


Fig 3.12. Alpha-diversity indices of the samples

Table 3.3. Summary of sequencing analysis of bacterial communities in the soil samples

Samples	OTUs^a	ACE	Jackknife	Chao 1	Phylogenetic diversity
Original	1834	1918	2018	1868	1926
Oxic 1	1088	1327	1373	1242	1615
Anoxic 2	962	1171	1223	1098	1450
Anoxic 3	1024	1081	1148	1055	1338
Anoxic 4	772	908	950	848	1121

a) Operational taxonomic units

Phylogenetic similarity was considered using Principal Component Analysis (PCA) to identify changes in soil microbial community. As a result, the microbial community was clearly distinguished by soil incubation and redox repetition. Principal component 1 and Principal component 2 accounted for 57.6 and 29.3% of the total data variance, respectively. The two main components preserved 86.9% of the total data variance and were sufficient to visualize two-dimensional visualization of soil microbial differences. As for Principal Component 1, soil microbial community showed significant difference according to soil incubation status. The value of original soil for Principal Component 1 was close to 0.5, whereas the

value of cultured soils (Oxic 1, Anoxic 2, Anoxic 3, Anoxic 4) was less than 0. Based on principal component 2, repetition of redox changes was an important variable. The values of Oxic 1 and Anoxic 2 soils were -0.14 and -0.20 for Principle 2, while the values of Anoxic 3 and Anoxic 4 soils were increased to 0.03 and 0.25, respectively. This means that the soil microbial composition gradually changed as the redox change was repeated. On the other hand, Anoxic 2, which is a reducing soil, and Oxic 1, which is an oxidizing soil, did not show significant differences based on both principal components 1 and 2. This means that redox repetition had a greater effect on the microbial community than the redox state itself.

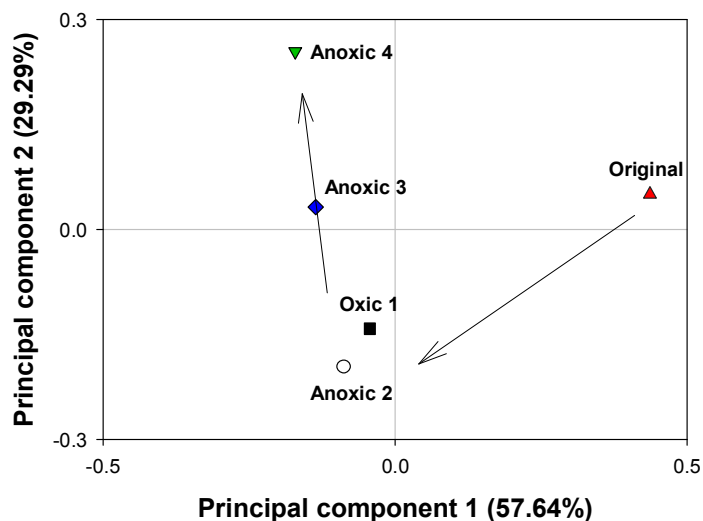


Fig 3.13. Principal component analysis of bacterial communities

4. Conclusions

Although As in soil can be released by reductive dissolution, it tends to be adsorbed again in aerobic condition, and the extent of adsorption increases as the cycle repeated. In the presence of an external carbon source, As(V) is further reduced to As(III), which makes As more mobile by inhibiting readsorption of As. Organic carbon source can be introduced into contaminated site by introduction of rainfall or groundwater fluctuation. Therefore, organic matter input is needed to be monitored carefully in As contaminated redox transition zone. Our findings show that soil iron oxides in redox transition zone are likely to transform to more amorphous form. This means that iron oxides can adsorb larger amounts of As under the oxic period, but can be more easily eluted during the anoxic period, resulting in higher As mobility.

As a result of bacterial community analysis, it was confirmed that the composition and diversity of bacterial community in As-contaminated soils were greatly changed by redox cycling. Repeated changes in redox conditions selectively increased abundance of bacterial species able to survive under both oxidizing and reducing conditions (e.g., *Azospirillum*), reducing the abundance of strict (an)aerobic microorganisms and consequently reducing

bacterial diversity. Under the reducing conditions, it was confirmed that various microorganisms (e.g., *Clostridium*, *Desulfitobacterium*) known to be capable of reducing Fe or As dominated. Among these, the *Clostridium beijerinckii* group made up the core bacterial community. The results of this study show that the bacterial community is dependent on the number of redox transitions. These findings would be helpful for selecting risk-management strategy in As-contaminated redox transition zone.

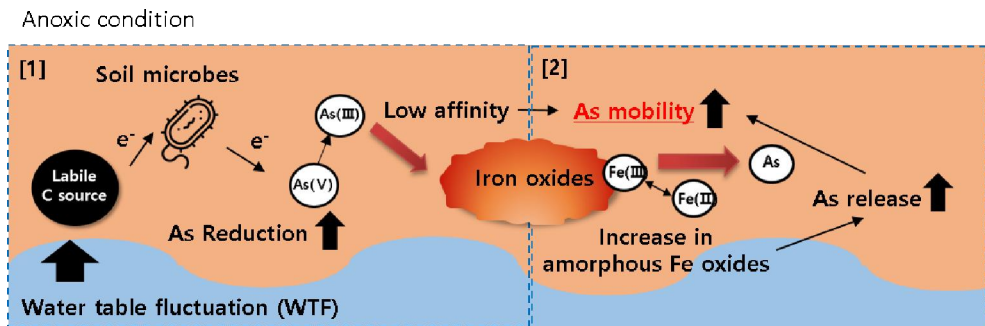


Fig 3.14. Increased mobility of As under anoxic condition in redox transition zones

Reference

Ahmed, B., et al. (2012). Fe (III) reduction and U (VI) immobilization by *Paenibacillus sp.* strain 300A, isolated from Hanford 300A subsurface sediments. *Appl. Environ. Microbiol* 78(22), 8001-8009.

Bachate, S., et al. (2009). Arsenic-resistant bacteria isolated from agricultural soils of Bangladesh and characterization of arsenate-reducing strains. *J. Appl. Microbiol.*, 107(1), 145-156.

Benz, M., et al. (1998). Humic acid reduction by *Propionibacterium freudenreichii* and other fermenting bacteria. *Appl. Environ. Microbiol.*, 64(11), 4507-4512.

Bishop, M. E., et al. (2019). Reactivity of redox cycled Fe-bearing subsurface sediments towards hexavalent chromium reduction. *Geochim. Cosmochim. Acta*, 252, 88-106.

Bissen, M. and F. H. Frimmel (2003). Hydrology: anthropogenic arsenic. *Nature Geoscience* 3(1), 5.

Boucher, D., et al. (2006). Succession of bacterial community composition over two consecutive years in two aquatic systems: a natural lake and a lake-reservoir. *FEMS Microbiol. Ecol.*, 55(1), 79-97.

Burnol, A., et al. (2007). Decoupling of arsenic and iron release from ferrihydrite suspension under reducing conditions: a biogeochemical model. *Geochemical Transactions* 8(1), 12.

Calatayud, M., J. et al. (2014). Trivalent arsenic species induce changes in expression and levels of proinflammatory cytokines in intestinal epithelial cells. *Toxicol. Lett.*, 224(1), 40-46.

Clague, J., et al. (2019). The influence of unsaturated zone drainage status on denitrification and the redox succession in shallow groundwater. *Sci. Total Environ.*, 660, 1232-1244.

Chen, Z., et al. (2016). Enhanced bioreduction of iron and arsenic in sediment by biochar amendment influencing microbial community composition and dissolved organic matter content and composition. *Journal of hazardous materials* 311, 20-29.

Couture, R. M., et al. (2015). On-off mobilization of contaminants in soils during redox oscillations. *Environmental Science & Technology* 49(5), 3015-3023.

D'Hondt, S., et al. (2004). Distributions of microbial activities in deep seafloor sediments. *Science*, 306(5705), 2216-2221.

de Zamaroczy, M., et al. (1989). Regulation of transcription and promoter mapping of the structural genes for nitrogenase (*nifHDK*) of *Azospirillum brasilense* Sp7. *Mol. Gen. Genet.*, 220(1), 33-42.

DeAngelis, K. M., et al. (2010). Microbial communities acclimate to recurring changes in soil redox potential status. *Environ. Microbiol.*, 12(12), 3137-3149.

Dobbin, P. S., et al. (1999). Dissimilatory Fe (III) reduction by *Clostridium beijerinckii* isolated from freshwater sediment using Fe (III)

maltol enrichment. FEMS Microbiol. Lett., 176(1), 131-138.

Dong, Y., et al. (2016). Hematite reduction buffers acid generation and enhances nutrient uptake by a fermentative iron reducing bacterium, *Orenia metallireducens* strain Z6. Environmental Science & Technology 51(1): 232-242.

Duan, Y., et al. (2019). Experimental constraints on redox-induced arsenic release and retention from aquifer sediments in the Central Yangtze River Basin. Science of the Total Environment 649, 629-639.

Falkowski, P. G., et al. (2008). The microbial engines that drive Earth's biogeochemical cycles. Science, 320(5879), 1034-1039.

Ferguson, J. F. and J. Gavis (1972). A review of the arsenic cycle in natural waters. Water research 6(11): 1259-1274.

Ginn, B., et al. (2017). Rapid iron reduction rates are stimulated by high-amplitude redox fluctuations in a tropical forest soil. Environmental Science & Technology 51(6): 3250-3259.

Han, Y. S., et al. (2019). Redox transformation of soil minerals and arsenic in arsenic-contaminated soil under cycling redox conditions. Journal of hazardous materials, 120745.

Harvey, C. F., et al. (2002). Arsenic mobility and groundwater extraction in Bangladesh. Science 298(5598), 1602-1606.

Hassan, Z., et al. (2015). Diverse arsenic-and iron-cycling microbial communities in arsenic-contaminated aquifers used for drinking

water in Bangladesh. FEMS microbiology ecology 91(4), fiv026.

Hong, H., et al. (2015). *Geosporobacter ferrireducens* sp. nov., an anaerobic iron-reducing bacterium isolated from an oil-contaminated site. Antonie van Leeuwenhoe 107(4), 971-977.

Huang, K., et al. (2018). Identification of hydro-geochemical processes controlling seasonal variations in arsenic concentrations within a riverbank aquifer at Jiangnan Plain, China. Water Resources Research.

Humans, I.W.G.o.t.E.o.C.R.t., et al. (2004). Some drinking-water disinfectants and contaminants, including arsenic, IARC.

Islam, F. S., et al. (2004). Role of metal-reducing bacteria in arsenic release from Bengal delta sediments. Nature, 430(6995), 68.

Jackson, C. R., et al. (2005). Enumeration and characterization of arsenate-resistant bacteria in arsenic free soils. Soil Biol. Biochem., 37(12), 2319-2322.

Jiang, S., et al. (2013). Differential arsenic mobilization from As-bearing ferrihydrite by iron-respiring *Shewanella* strains with different arsenic-reducing activities. Environ. Sci. Technol., 47(15), 8616-8623.

Jung, H. B., et al. (2015). Redox zonation and oscillation in the hyporheic zone of the Ganges-Brahmaputra-Meghna Delta: implications for the fate of groundwater arsenic during discharge. Appl. Geochem., 63, 647-660.

Kim, E. J., et al. (2014). Arsenic speciation and bioaccessibility in

arsenic-contaminated soils: sequential extraction and mineralogical investigation. *Environmental pollution* 186: 29-35.

Kingston, H. and Walter, P. (1988). Method 3052 – Microwave assisted acid digestion of siliceous and organically based matrices. EPA IAG#DWI – 393254-01-0 January.

Kocar, B. D., et al. (2006). Contrasting effects of dissimilatory iron (III) and arsenic (V) reduction on arsenic retention and transport. *Environmental Science & Technology* 40(21): 6715-6721.

Lara, J., et al. (2012). Enrichment of arsenic transforming and resistant heterotrophic bacteria from sediments of two salt lakes in Northern Chile. *Extremophiles*, 16(3), 523-538.

Lee, C. W., et al. (2019). Bioimaging: New Templated Ostwald Ripening Process of Mesostructured FeOOH for Third Harmonic Generation Bioimaging. *Small* 15(20): 1970108.

LeMonte, J. J., et al. (2017). Sea level rise induced arsenic release from historically contaminated coastal soils. *Environmental Science & Technology* 51(11), 5913-5922.

Li, L., et al. (2017). Excessive input of phosphorus significantly affects microbial Fe (III) reduction in flooded paddy soils by changing the abundances and community structures of Clostridium and Geobacteraceae. *Science of the total environment* 607: 982-991.

Lin, Z., et al. (2018). Nitrate reduced arsenic redox transformation and transfer in flooded paddy soil-rice system. *Environ. Pollut.*, 243, 1015-

1025.

Lindsay, W. (1991). Iron oxide solubilization by organic matter and its effect on iron availability. Iron nutrition and interactions in plants, Springer: 29-36.

List, C., et al. (2019). Impact of iron reduction on the metabolism of *Clostridium acetobutylicum*. Environmental microbiology.

Livesey, N. T., and Huang, P. M. (1981). Adsorption of arsenate by soils and its relation to selected chemical properties and anions. Soil Science 131, 88-94.

Loeppart, R. H., Inskeep, W. P. (1996). In Methods of Soil Analysis. Part 3. Chemical Methods; Sparks, D. L., Ed; Soil Science Society of America: Madison, WI, 384-411.

Loreau, M. (2001). Microbial diversity, producer–decomposer interactions and ecosystem processes: a theoretical model. Proc. R. Soc. London, Ser. B, 268(1464), 303-309.

Lovley, D. (2006). Dissimilatory Fe (III)-and Mn (IV)-reducing prokaryotes. The Prokaryotes: Volume 2: Ecophysiology and Biochemistry, 635-658.

Mandal, B. K. and K. T. Suzuki (2002). Arsenic round the world: a review. Talanta, 58(1), 201-235.

Manning, B. (2005) Arsenic speciation in As (III)–and As(V)–treated soil using XANES spectroscopy. Microchimica Acta 151(3-4), 181-

188.

Mejia, J., et al. (2016). Influence of oxygen and nitrate on Fe (hydr) oxide mineral transformation and soil microbial communities during redox cycling. *Environmental science & technology* 50(7), 3580-3588.

Meng, X., R. R. et al. (2017). Mineralogy and geochemistry affecting arsenic solubility in sediment profiles from the shallow basin-fill aquifer of Cache Valley Basin, Utah. *Appl. Geochem.*, 77, 126-141.

Möller, L., P. et al. (2019). *Sulfurimonas* subgroup GD17 cells accumulate polyphosphate under fluctuating redox conditions in the Baltic Sea: possible implications for their ecology. *The ISME journal*, 13(2), 482.

Moon, H. S., et al. (2017). Effect of the redox dynamics on microbial-mediated As transformation coupled with Fe and S in flow-through sediment columns. *Journal of Hazardous Materials* 329, 280-289.

Muntau, M., M. et al. (2017). Evaluation of the short-term fate and transport of chemicals of emerging concern during soil-aquifer treatment using select transformation products as intrinsic redox-sensitive tracers. *Sci. Total Environ.*, 583, 10-18.

Murphy, J. and J. P. Riley (1962). A Modified single solution method for the determination of phosphate in natural waters. *Analytica chimica acta* 27, 31-36.

Newman, D. K. and J. F. Banfield. (2002). Geomicrobiology: how molecular-scale interactions underpin biogeochemical systems. *Science* 296(5570), 1071-1077.

Noël, V., et al. (2019). Uranium storage mechanisms in wet-dry redox cycled sediments. *Water research* 152, 251-263.

Oliveira, A., M. et al. (2009). Enumeration and characterization of arsenic-tolerant diazotrophic bacteria in a long-term heavy-metal-contaminated soil. *Water, Air, Soil Pollut.*, 200(1-4), 237-243.

Oremland, R. S. and Stolz, J. F. (2005) Arsenic, microbes and contaminated aquifers. *Trends in Microbiology* 13(2), 45-49.

Pan, Y., et al. (2017). The role of enriched microbial consortium on iron-reducing bioaugmentation in sediments. *Frontiers in Microbiology* 8, 462.

Park, J. H., et al. (2018). Mobility of multiple heavy metalloids in contaminated soil under various redox conditions: Effects of iron sulfide presence and phosphate competition, *Chemosphere*, 197, 344-352.

Parsons, C. T., et al. (2013). The impact of oscillating redox conditions: arsenic immobilisation in contaminated calcareous floodplain soils. *Environmental pollution* 178, 254-263.

Paul, S., S. Majumdar and A. K. Giri (2015). Genetic susceptibility to arsenic-induced skin lesions and health effects: a review. *Gene. Environ.*, 37(1), 23.

Qiao, J.-t., et al. (2018). Roles of different active metal-reducing bacteria in arsenic release from arsenic-contaminated paddy soil amended with biochar. *Journal of hazardous materials* 344, 958-967.

Rakhimbekova, S., et al. (2018). Effect of transient wave forcing on

the behavior of arsenic in a nearshore aquifer. *Environmental Science & Technology* 52(21). 12338-12348.

Ravel, B. and Newville, M. (2005). ATHENA, ARTEMIS, HEPHAESTUS: data analysis for X-ray absorption spectroscopy using IFFEFFIT. *Journal of synchrotron radiation* 12(4), 537-541.

Ray, A. E., et al. (2018). Metal transformation by a novel *Pelosinus* isolate from a subsurface environment. *Frontiers in microbiology* 9.

Roberts, L. C., et al. (2010). Arsenic release from paddy soils during monsoon flooding. *Nature Geoscience* 3(1), 53.

Rodriguez-Mora, M. J., et al. (2015). The dynamics of the bacterial diversity in the redox transition and anoxic zones of the Cariaco Basin assessed by parallel tag sequencing. *FEMS Microbiol. Ecol.*, 91(9), fiv088.

Schwertmann, R. Cornell. (2008). *Ferrihydrite, Iron oxides in the laboratory: Preparation and characterization*, Wiley-VCH, Weinheim

Shade, A. and J. Handelsman. (2012). Beyond the Venn diagram: the hunt for a core microbiome. *Environmental microbiology* 14(1), 4-12.

Smedley, Pauline L and Kinniburgh, DG. (2002). A review of the source, behavior and distribution of arsenic in natural waters. *Applied Geochemistry* 17(5), 517-568.

Sparks, D. L., Helmke, P., and Page, A. (1996). *Methods of soil analysis: Chemical methods*. Retrieved from

Sposito, G. (2008). *The chemistry of soils*: Oxford university press.

Stern, N., et al. (2018). Dual role of humic substances as electron donor and shuttle for dissimilatory iron reduction. *Environmental Science & Technology* 52(10), 5691-5699.

Stookey, L. L. (1970). Ferrozine – a new spectrophotometric reagent for iron. *Analytical Chemistry* 42(7), 779-781.

Teh, Y. A., et al. (2005). Oxygen effects on methane production and oxidation in humid tropical forest soils. *Global Change Biol.*, 11(8), 1283-1297.

Thompson, A., et al. (2006). Iron-oxide crystallinity increases during soil redox oscillations. *Geochimica et Cosmochimica Acta* 70(7), 1710-1727.

Thouin, H., et al. (2018). Influence of environmental changes on the biogeochemistry of arsenic in a soil polluted by the destruction of chemical weapons: A mesocosm study. *Science of the Total Environment* 627, 216-226.

Torsvik, V. and L. Øvreås (2002). Microbial diversity and function in soil: from genes to ecosystems. *Curr. Opin. Microbiol.*, 5(3), 240-245.

Waldrop, M. and M. Firestone (2006). Seasonal dynamics of microbial community composition and function in oak canopy and open grassland soils. *Microb. Ecol.*, 52(3), 470-479.

Wang, N., X.-M. et al. (2017). Biochar increases arsenic release from an anaerobic paddy soil due to enhanced microbial reduction of iron and arsenic. *Environ. Pollut.*, 220, 514-522.

Wang, X.-J., J. et al. (2009). Phylogenetic diversity of dissimilatory ferric iron reducers in paddy soil of Hunan, South China. *J. Soils Sed.*, 9(6), 568-577.

Wang, Y., et al. (2016). Release and transformation of arsenic from As-bearing iron minerals by Fe-reducing bacteria. *Chem. Eng. J.*, 295, 29-38.

Weingarden, A., et al. (2015). Dynamic changes in short-and long-term bacterial composition following fecal microbiota transplantation for recurrent *Clostridium difficile* infection. *Microbiome* 3(1), 10.

Wenzel, W. W., et al. (2001). Arsenic fractionation in soils using an improved sequential extraction procedure. *Analytica Chimica Acta* 436(2), 309-323.

Winkel, L., M. et al. (2008). Predicting groundwater arsenic contamination in Southeast Asia from surface parameters. *Nature Geoscience*, 1(8), 536.

Xie, Z., J. et al. (2018). Interactions between arsenic adsorption/desorption and indigenous bacterial activity in shallow high arsenic aquifer sediments from the Jiangnan Plain, Central China. *Sci. Total Environ.*, 644, 382-388.

Yang, Y.-P., et al. (2018). Microbe mediated arsenic release from iron minerals and arsenic methylation in rhizosphere controls arsenic fate in soil-rice system after straw incorporation. *Environ. Pollut.*, 236, 598-608.

Ye, Chen, et al. (2015). Revegetation impacts soil nitrogen dynamics in the water level fluctuation zone of the Three Gorges Reservoir, China.

Science of the Total Environment 517, 76-85.

Yoon, Y., et al. (2016). Comparative evaluation of magnetite–graphene oxide and magnetite-reduced graphene oxide composite for As (III) and As (V) removal. *Journal of hazardous materials* 304: 196-204.

Zhao, R., B. et al. (2019). Nitrifier abundance and diversity peak at deep redox transition zones. *Scientific reports*, 9(1), 8633.

초 록

Redox Transition Zone 토양에서 유기물 유입과 철산화물의 성질 변화가 비소의 이동성에 주는 영향

서울대학교 대학원

건설환경공학부

박수진

수리학적 경계가 고정되지 않은 부지에서는 산화-환원 조건이 지속적으로 변화하고, 이는 토양 내 지구생화학적 반응에 중대한 영향을 준다. 비소는 산화-환원 조건에 민감한 오염물질로, Redox transition zone에서 이동성이 지속적으로 변화한다. 산화-환원 조건이 변화하는 토양에서 지하수로 비소가 용출되는 현상은

남아시아를 비롯한 전세계적으로 심각한 문제이나, 현재까지 반복적인 산화-환원 조건에서 비소 이동성의 경향이 어떻게 변화하는지에 관한 연구는 거의 수행되지 않았다. 본 연구에서는, batch incubation 실험을 통하여 redox transition zone에서 비소 이동성에 영향을 주는 생화학적 반응을 해석하는 것을 목표로 하였다. 비소는 미생물에 의한 철산화물 환원에 의해 용출되므로, 토양 철산화물의 결정화도, 비소의 산화 수, 그리고 토양 미생물 군집을 비소 이동성에 영향을 미치는 주요 요인으로 설정하고 평가하였다. 가장 먼저, 유기 탄소원 (포도당) 이 비소의 화학종에 미치는 영향을 분석하였다. 실험 결과, 환원 조건에서 비소는 미생물에 의한 철산화물의 환원 작용에 의하여 용출되었고, 이어지는 산화 조건에서 다시 토양에 흡착하였다. 그리고 흡착량은 산화-환원 조건이 반복됨에 따라 증가하였다. 용액 중에 존재하는 비소의 비율은 첫 산화 조건에서 전체의 25.2%이던 것이 마지막 산화 조건에서는 11.9%로 감소하였다. 그러나, 포도당이 중간에 첨가된 경우에는 용액 중 5가 비소가 감소하며 비소의 흡착량이 감소하였다. 3가 비소는 5가 비소와 비교하여 철산화물을 비롯한 광물에 흡착하는 정도가 낮으므로, 이는 유기탄소원이 용액 중 비소의 산화수에 영향을 주며 비소의 흡착을 저해했음을 의미한다. 철산화물의 성질 변화는 XANES-LCF 분석 및 선별추출을 이용하여

분석하였다. 토양 철산화물 중 대표적인 비결정질 철산화물인 ferrihydrite의 비율은 세 번의 redox 변화 이후 29.3%로 증가하였다. 선별추출 결과 DCB 용액에 의해 추출 가능한 (비결정질 또는 결정질인) 철의 양은 일정하게 유지된 반면, AAO 용액에 의해 용출 가능한 (비결정질 또는 반응성이 높은) 철의 양은 1.4에서 3.2 mg/g으로 증가하였다. 이는 산화-환원 조건의 변화가 반복되며 철산화물이 비결정질로 성질이 변화하였음을 의미한다. 비결정질 철산화물은 표면적과 용해도가 상대적으로 높아 미생물에 의해 촉진되는 reductive dissolution 작용에 취약하기 때문에, 철산화물의 비결정질화는 환원 조건에서 비소의 용출량을 증가시킬 수 있다. 토양 미생물 군집은 Illumina 시퀀싱으로 분석하였다. Illumina 시퀀싱 결과, 토양 미생물 군집은 redox 변화에 반응하며 변화하였다. 절대 호기성 또는 혐기성 미생물의 비율은 점차 감소한 반면, 미호기성 속인 *Azospirillum*은 incubation 종료 시 전체 미생물의 72.8%를 차지하며 우점하는 속이 되었다. 철/비소 환원이 가능한 *Clostridium*과 *Desulfitobacterium* 등의 토착 미생물이 발견되어 미생물에 의하여 철/비소의 환원이 촉진되었을 가능성을 확인하였다. 결과적으로, redox transition zone에서는 반복적인 redox 환경의 변화로 유기탄소원의 유입과 철산화물의 성질 변화가 발생할 수 있고, 이는 토양 내 지구화학적 반응에 영향을 주어 비소의 이동성과 독성을

증가시킨다. 따라서 본 연구결과는 비소로 오염된 redox transition zone을 관리하기 위해서는 장기적 모니터링이 필요함을 시사한다.

주요어: Redox transition zone, 비소 용출, 비결정질 철산화물, 철 환원

학 번: 2018-22553